

Supporting Information

Hybrid membranes of metal-organic molecule nanocages for aromatic/aliphatic hydrocarbon separation by pervaporation

Cui Zhao, Naixin Wang, Lin Wang, Hongliang Huang, Rong Zhang, Fan Yang, Yabo Xie, Shulan Ji,* Jian-Rong Li*

Beijing Key Laboratory for Green Catalysis and Separation and Department of Chemistry and Chemical Engineering, College of Environmental and Energy Engineering, Beijing University of Technology, Beijing 100124, P. R. China.

E-mail: jrli@bjut.edu.cn

1. Experimental details

1.1. Synthesis of MOP-*t*Bu

All the general reagents and solvents were commercially available and used as received. The MOP-*t*Bu was prepared according to our published procedure. An N,N-dimethylacetamide (DMA) solution (20 mL) of H₂(5-*t*Bu-1,3-BDC), (445 mg) was mixed with a DMA solution (20 mL) of Cu₂(OAc)₄·H₂O (400 mg) in a glass vial (50 mL) and stirred for 30 min at room temperature. After that, to this solution 10 mL of MeOH was added and then allowed the vial stand at room temperature. Finally, homogeneous dark-blue block crystals were collected and washed with MeOH solvent.

1.2. Preparation of pure W3000 and MOP-*t*Bu/W3000 tubular membranes

To prepare the pure W3000 and MOP-*t*Bu/W3000 membranes, the ceramic tube was modified using 3-aminopropyltriethoxysilane (APTES) as covalent linkers in

order to increase the adhesion force between the separation layer and Al₂O₃ support. In order to explore the optimal hybrid experimental condition, firstly, we prepared different concentrations of pure Boltorn W3000 membrane at different experimental conditions. The hybrid membrane forming process is the same with that of the pure W3000 membrane. In the hybrid membrane forming process, both HBP Boltorn W3000 and MOP-*t*Bu were first dissolved in N-Methyl pyrrolidone (NMP) solvent by stirring it to achieve transparent membrane-forming solution at room temperature. Subsequently, the pretreated ceramic tube was immersed in the prepared solution for 30 min and thermo-crosslinking at 150 °C for 2 h. This immersion and thermo-crosslinking processes were repeated to produce integrated membranes with different layers. Mixed matrix membranes with different MOP-*t*Bu loadings (1.6 wt%, 3.2 wt%, 4.8 wt%, 6.5 wt% and 13 wt%) were prepared. Finally the as-prepared membranes were preserved in air for further use.

1.3. Characterizations

The surface and cross-section morphologies of the prepared membranes were observed by SEM (Model SU8020, Hitachi, Japan). All membrane samples were dried under vacuum. Attenuated total reflection FTIR spectroscopy was performed on a Vertex-70 spectro photometer (Bruker, Germany) to characterize the morphological changes of the nanohybrid membrane. The powder X-ray diffraction patterns (PXRD) were recorded on a BRUKER D8-Focus Bragg-Brentano X-ray Powder Diffractometer equipped with a Cu sealed tube ($\lambda = 1.54178$) at room temperature. Thermo gravimetric analysis (TGA) experiments were carried out at a heating rate of 10 °C/min under nitrogen, using a TGA thermo gravimetric analyzer. X-ray photoelectron spectroscopy data were obtained using an ESCALab250 electron spectrometer from Thermo Scientific Corporation with monochromatic 150 W AlK α radiation. The depth profiles of the concentrations of Si, N, C, Cu, and O in the membrane were obtained from the C1s, Si2p, O1s and Cu2p energy bands by sputtering with 1 kV and 1 uA at 6 nm/min, with the etching area of 3 mm \times 3 mm.

The as-prepared nanohybrid membranes were evaluated using a pervaporation cell fabricated in our laboratory with an effective area of 26 cm².¹ The permeate vapor was trapped in liquid nitrogen. For each pervaporation run, the membrane was subjected to 2 h conditioning to ensure that the membrane reached a steady state before sample collection. The permeate sample was collected at 2 h intervals. Three

samples were collected for measurements. The experiments were carried out at a downstream pressure of 100 Pa, which was maintained by a vacuum pump. Fluxes were determined by measuring the weight of the liquid collected in the cold traps at specific times under steady-state conditions. The composition of the collected permeating fluid was determined by gas chromatography (FULI 979011, China). The separation factor was calculated according to the following equation:

$$\alpha = \frac{Y_i / Y_j}{X_i / X_j}$$

Where, Y_i and Y_j represent the mass fraction of toluene (or benzene) and n-heptane (or cyclohexane) in the permeating fluid, respectively; X_i and X_j represent the mass fraction of toluene (or benzene) and n-heptane (or cyclohexane) in the feed, respectively.

2. Additional tables and figures

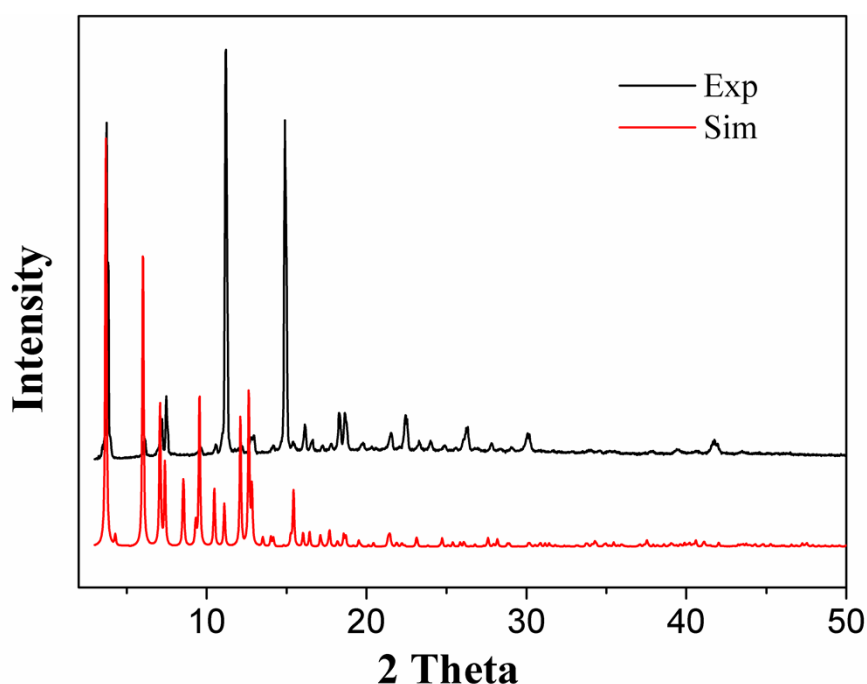


Fig. S1. PXRD patterns of as-synthesized MOP-*t*Bu and simulated on its single-crystal data.

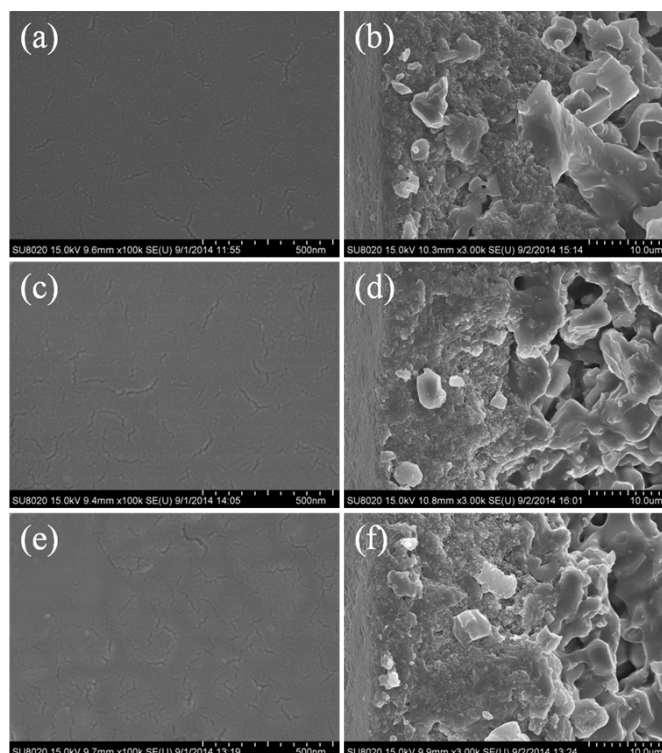


Fig. S2. SEM images of (a) surface of $\text{Al}_2\text{O}_3/\text{W3000}$ membrane (100 k) (15 wt% concentration of W3000, two layers), (b) cross-section of $\text{Al}_2\text{O}_3/\text{W3000}$ membrane (3 k), (15 wt% concentration of W3000, two layers), (c) surface of $\text{Al}_2\text{O}_3/\text{MOP-}t\text{Bu}/\text{W3000}$ membrane (100 k) (1.6 wt% MOP-*t*Bu loading, 15 wt% concentration of W3000, two layers), (d) cross-section of $\text{Al}_2\text{O}_3/\text{MOP-}t\text{Bu}/\text{W3000}$ membrane (100 k) (1.6 wt% MOP-*t*Bu loading, 15 wt% concentration of W3000, two layers), (e) surface of $\text{Al}_2\text{O}_3/\text{MOP-}t\text{Bu}/\text{W3000}$ membrane (100 k) (13 wt% MOP-*t*Bu loading, 15 wt% concentration of W3000, two layers), and (f) cross-section of $\text{Al}_2\text{O}_3/\text{MOP-}t\text{Bu}/\text{W3000}$ membrane (3 k) (13 wt% MOP-*t*Bu loading, 15 wt% concentration of W3000, two layers).

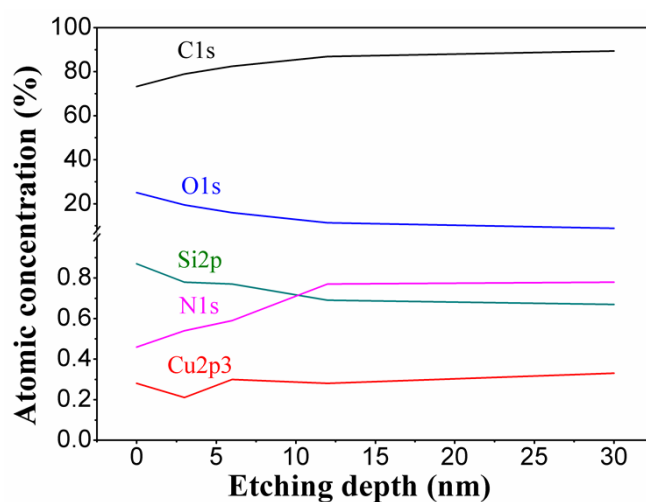


Fig. S3. XPS depth profiles of C1s, O1s, Si2p, N1s, and Cu2p3 in the MOP-*t*Bu/W3000 hybrid membrane.

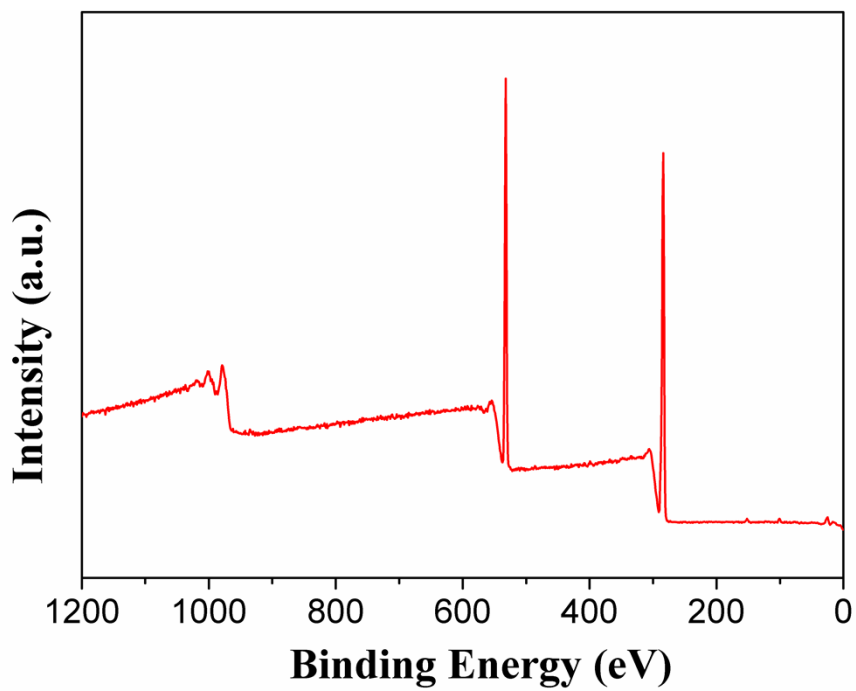


Fig. S4. XPS of the surface of the MOP-*t*Bu/W3000 hybrid membrane.

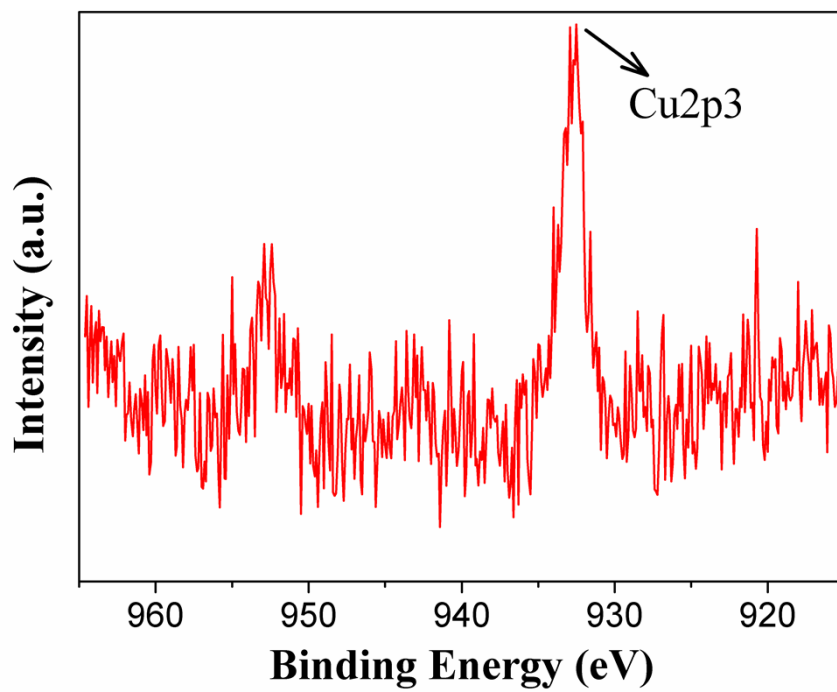


Fig. S5. The enlarged XPS for Cu2p3 site.

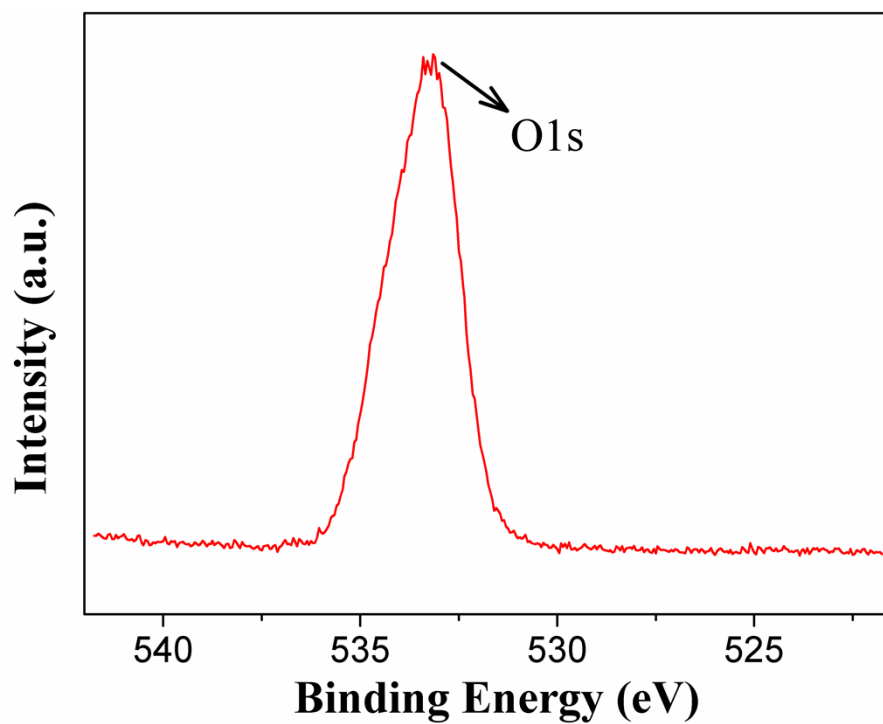


Fig. S6. The enlarged XPS for O1s site.

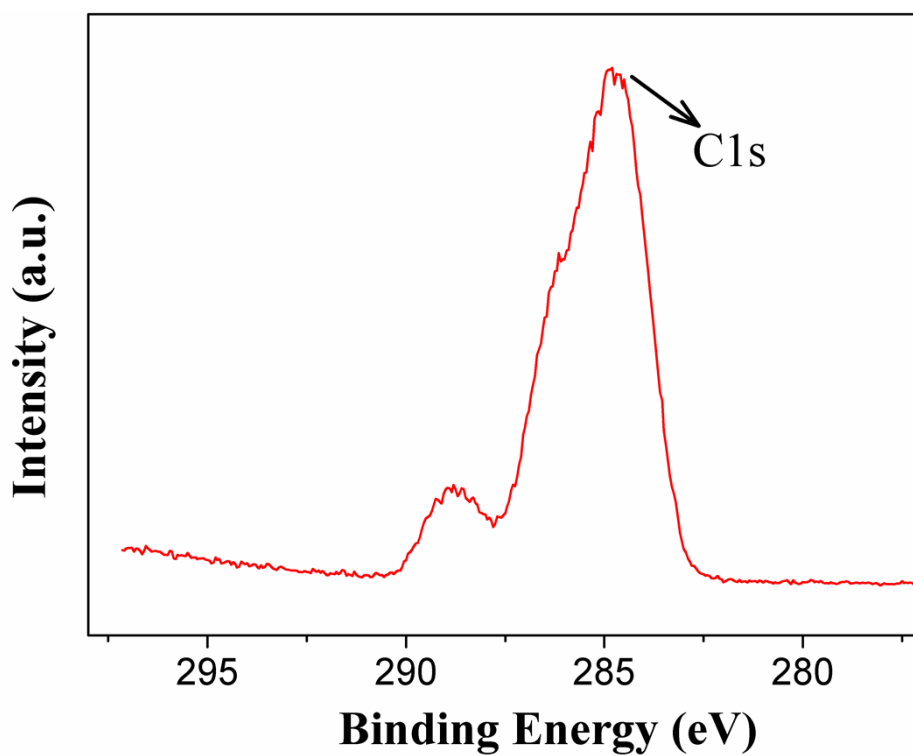


Fig. S7. The enlarged XPS for C1s site.

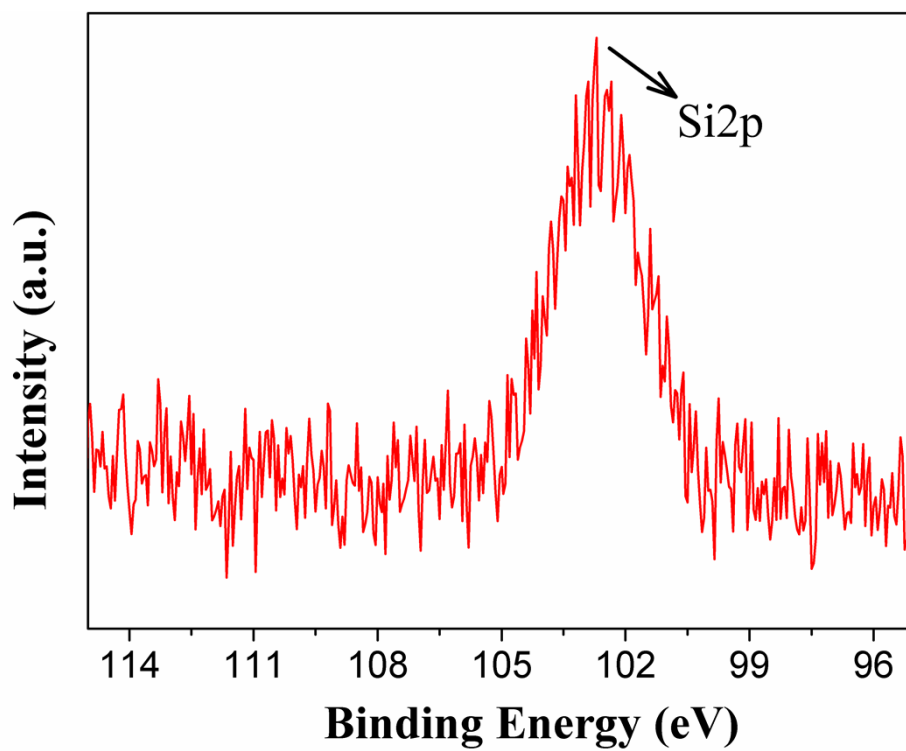


Fig. S8. The enlarged XPS for Si2p site.

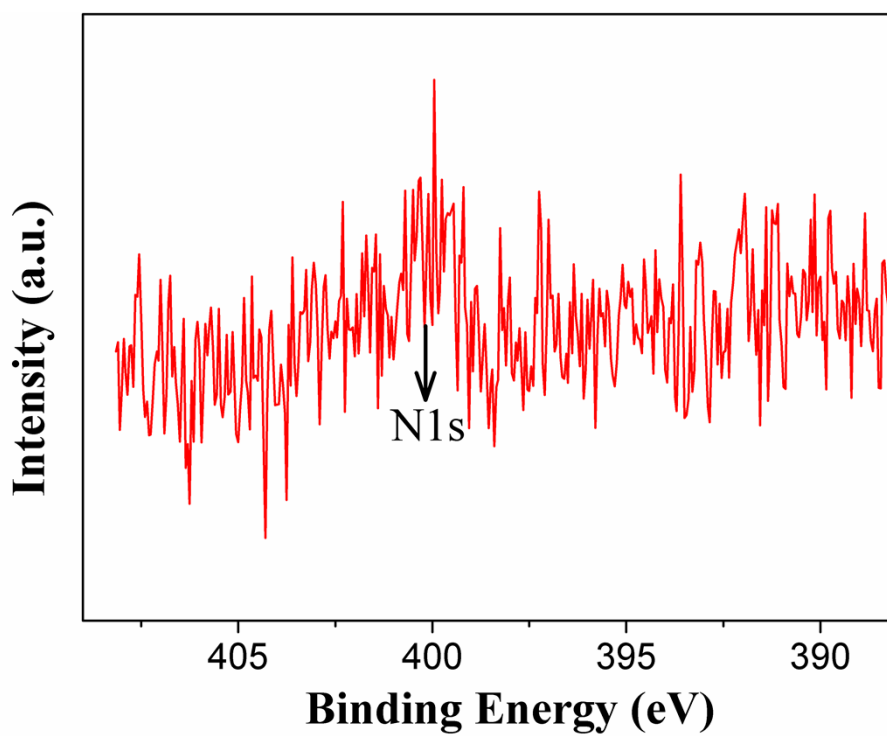


Fig. S9. The enlarged XPS for N1s site.

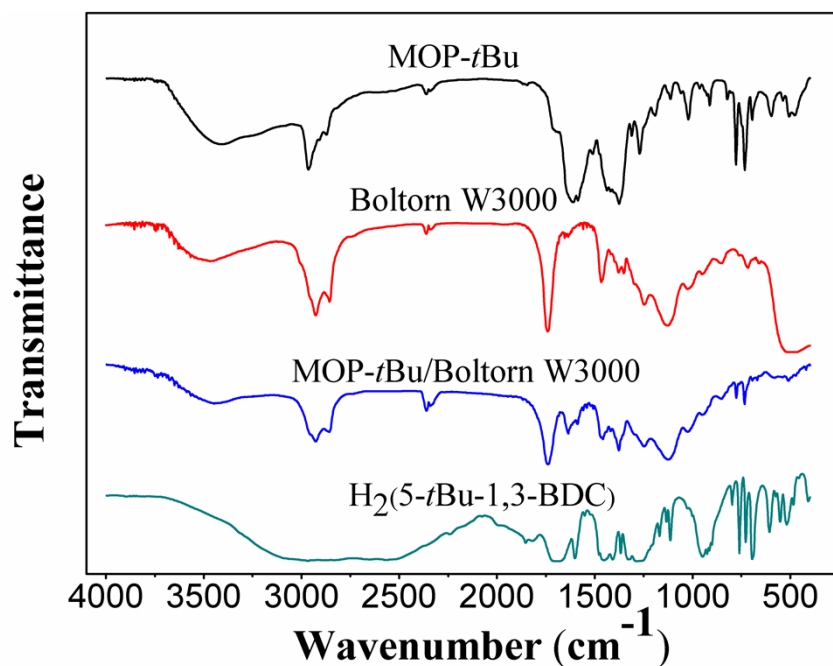


Fig. S10. ATR-FTIR spectra of MOP-*t*Bu, H₂(5-*t*Bu-1,3-BDC), pure Boltorn W3000 membrane (preparation conditions: immersion time, 30 min; thermal-crosslinking temperature, 150 °C; 15 wt% Boltorn W3000 NMP solution) and thermal cross-linked MOP-*t*Bu/Boltorn W3000 hybrid membrane with 13 wt% loading (preparation conditions: immersion time, 30 min; thermal-crosslinking temperature, 150 °C; 15 wt% Boltorn W3000 NMP solution; 15 wt% Boltorn W3000 NMP solution with 13 wt% MOP-*t*Bu loading).

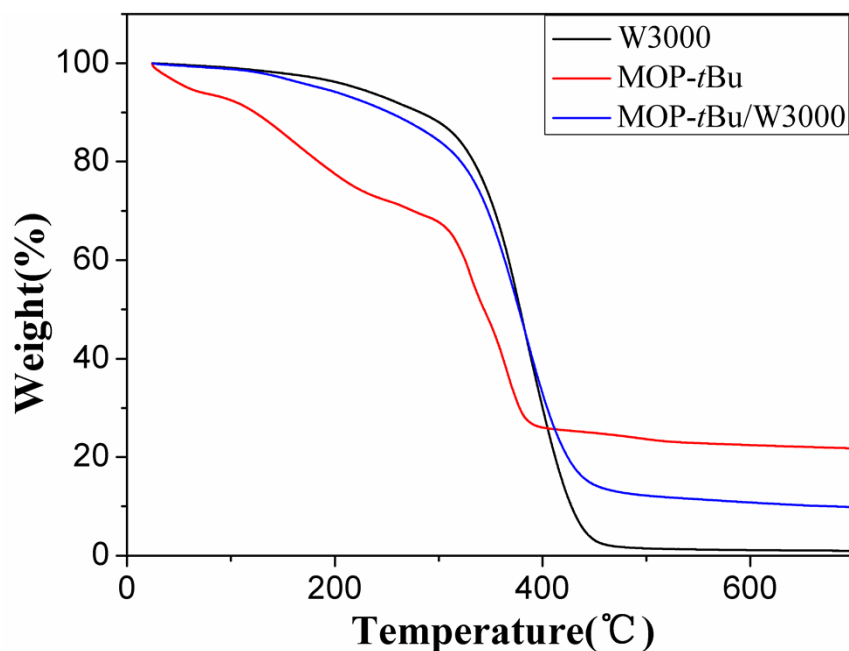


Fig. S11. TGA curves of MOP-*t*Bu, pure Boltorn W3000, and MOP-*t*Bu/W3000 hybrid with 13 wt% MOP-*t*Bu loading.

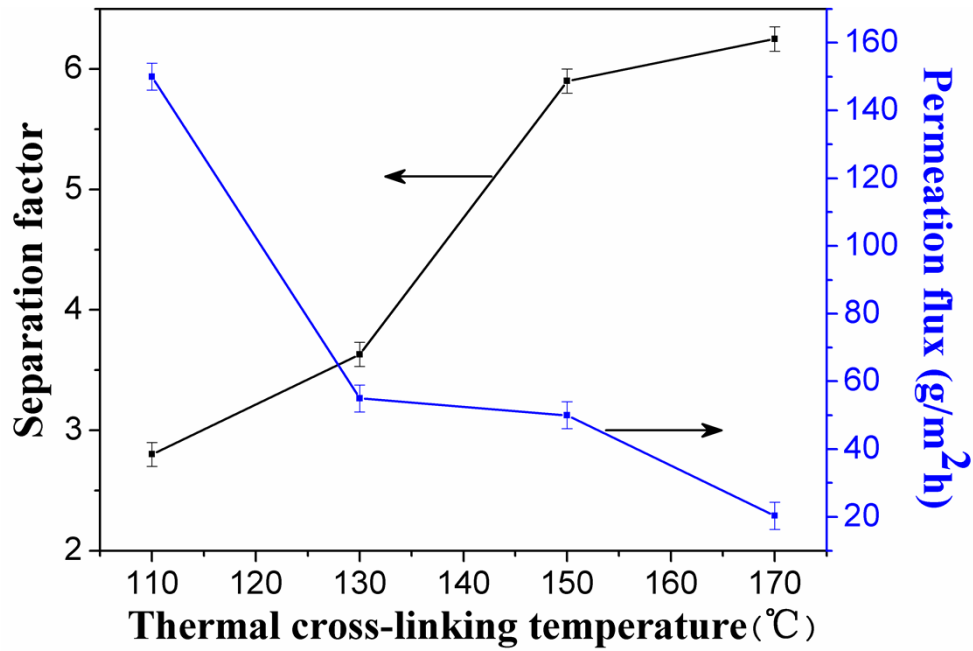


Fig. S12. Effects of thermal-crosslinking temperature on the pervaporation performances of the pure Boltorn W3000 membrane (Preparation conditions: immersion time, 30 min and concentration of Boltorn W3000, 15 wt%).

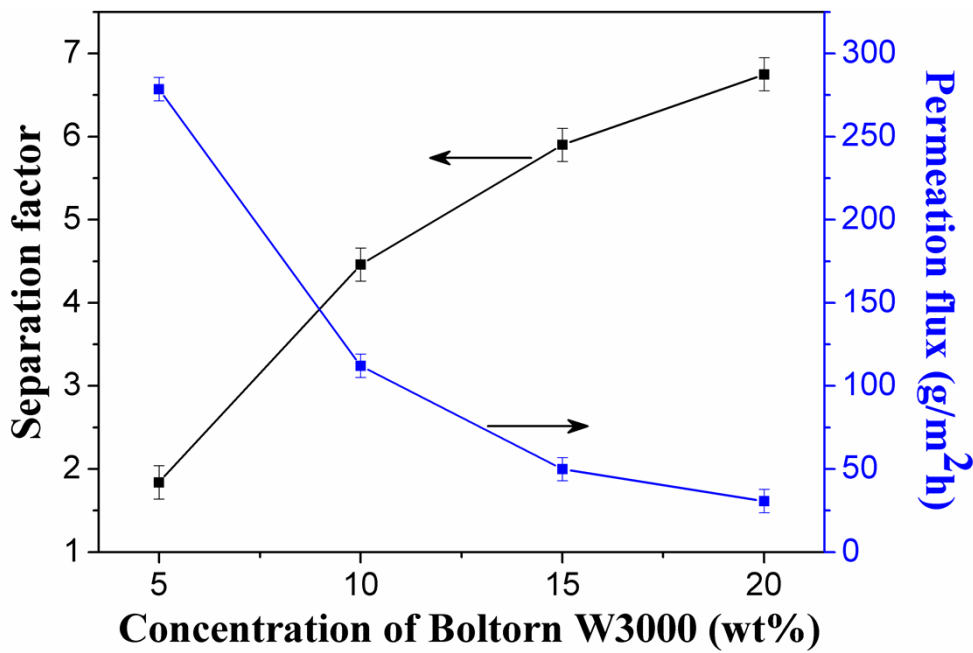


Fig. S13. Effects of Boltorn W3000 concentrations on pervaporation performances (Preparation conditions: immersion time, 30 min and thermal-crosslinking temperature, 150 °C).

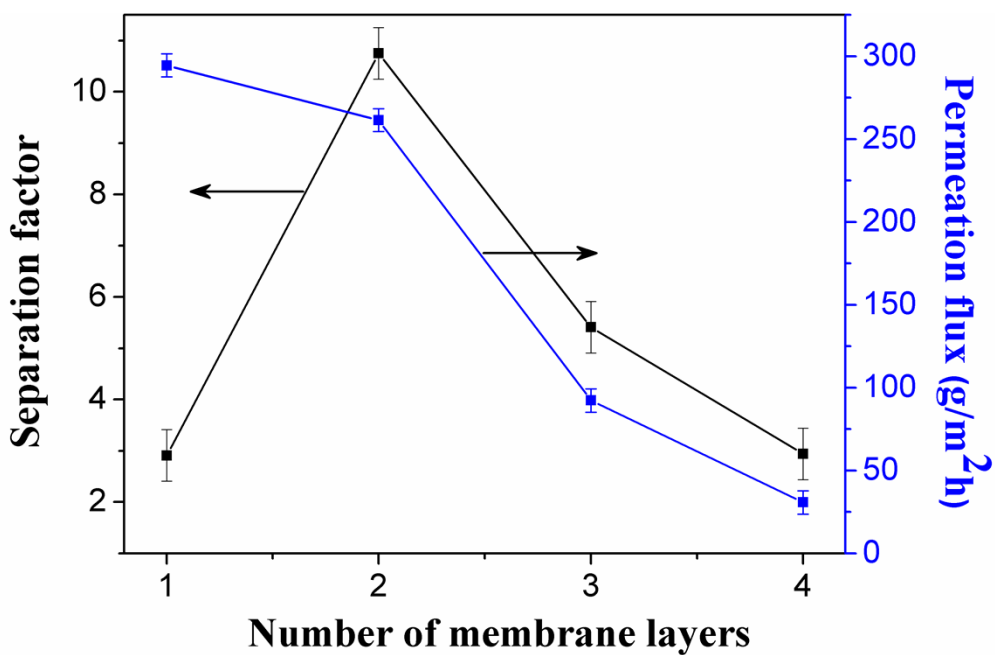


Fig. S14. Effects of layer number on pervaporation performances of the MOP-*t*Bu/W3000 hybrid membrane (Preparation conditions: concentration of Boltorn W3000, 15 wt%; MOP-*t*Bu loading, 6.5 wt%; immersion time, 30 min; and thermal-crosslinking temperature, 150 °C).

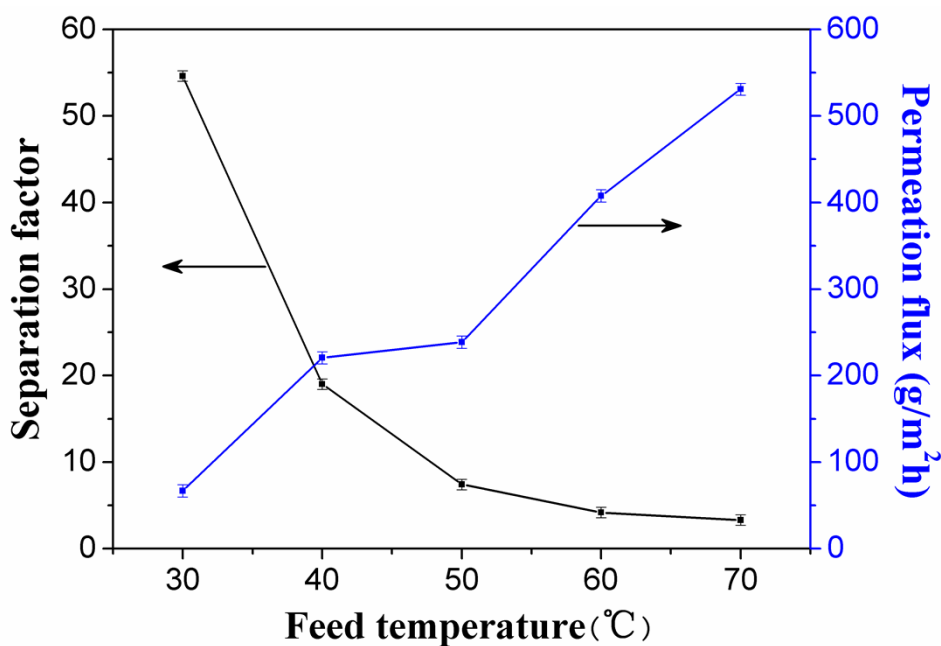


Fig. S15. Effects of feed temperature on pervaporation performances of the MOP-*t*Bu/W3000 hybrid membrane (Preparation conditions: concentration of Boltorn W3000, 15 wt%; MOP-*t*Bu loading, 4.8 wt%; immersion time, 30 min; thermal-crosslinking temperature, 150 °C; and number of membrane layers, 2).

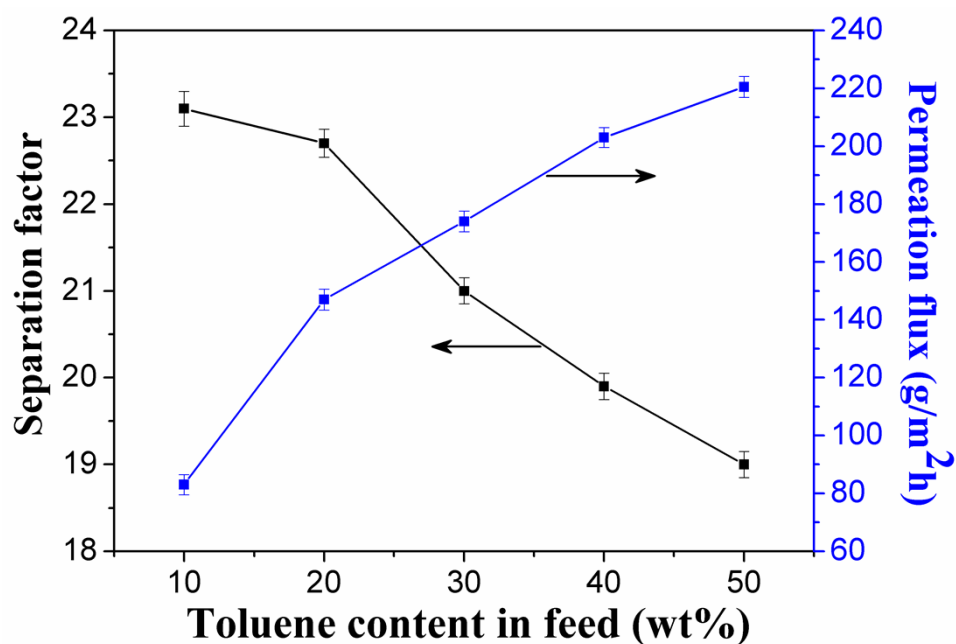


Fig. S16. Effects of toluene content in feed solution on pervaporation performances of MOP-*t*Bu/W3000 hybrid membrane (Preparation conditions: concentration of Boltorn W3000, 15 wt%; MOP-*t*Bu loading, 4.8 wt%; immersion time, 30 min; thermal-crosslinking temperature, 150 °C; and number of membrane layers, 2).

Table S1. Pervaporation performances of some membranes in the separation of toluene/*n*-heptane mixture in this work and literatures.

Membrane	Feed concentration wt% (toluene)	Feed temperature / °C	Total flux /g/m ² h	Separation factor	Ref.
PAN/poly(ethylene glycol) methacrylate	25	80	1620	7.8	2
Aromatic polyimide and polybenzoxazole	40	80	15-46	4.7	2
FDA-DSDA	40.9	80	15-46.15	8.1	3
4MPD-BTDA	39.1	80	229.5-706	6.0	3
1.6 wt% SEC + NaDDS	18.9	80	980	4.2	4
PEO360OHMA	20.2	80	290	6.6	4
PAN/p-(MMA-co-MASPE)/BDDDMAC	20	80	1070	4.7	4
PEO400OHMA	20.1	80	1100	6.7	5
FDA/ATPEPG(30:70)-BTDA	20.2	60	115	6.8	6

FDA-BTDA	41.3	80	54.16	7.0	6
Polyethylene glycol dimethacrylate/acrylate d cyclodextrins	10	60	4.3-7.5	14	7
PAN/PVA	50	40	42.4	4.5	8
PAN/PVA-GO	50	40	27	12.9	8
MOP- <i>t</i> Bu/W3000	50	40	220	19	This work
MOP- <i>t</i> Bu/W3000	50	30	66.7	54.6	This work

Table S2. Pervaporation performances of some membranes in the separation of benzene/cyclohexane mixture in this work and literatures.

Membrane	Feed concentration wt.%(benzene)	Feed temperature /°C	Total flux /g/m ² h	Separation factor	Ref.
PANPMA	50	30	1.17	10.5	9
F8	13.3	30	14.26	212	10
F0	13.3	30	30.8	88.7	10
PEA	50	50	14.76	7.1	10
PEMA-EGDM	10	40	3.8	6.7	11
PU(0)-650	54	25	1142-2284	2.7	12
PVA-GPTMS-28	50	50	137.1	46.9	13
β-CD/PVA/GA	50	50	30.9	27	14
PVA-graphite	50	50	91.3	91.6	15
MOP- <i>t</i> Bu/W3000	50	30	392.3	15.4	This work

References:

1. N. Wang, S. Ji, G. Zhang, J. Li and L. Wang, *Chem. Eng. J.*, 2012, **213**, 318.
2. Z. Li, B. Zhang, L. Qu, J. Ren and Y. Li, *J. Membr. Sci.*, 2011, **371**, 163.
3. C. P. Ribeiro, B. D. Freeman, D. S. Kalika and S. Kalakkunnath, *J. Membr. Sci.*, 2012, **390-391**, 182.
4. H. H. Schwarz and G. Malsch, *J. Membr. Sci.*, 2005, **247**, 143.

5. J. Frahn, G. Malsch, H. Matuschewski, U. Schedler and H. H Schwarz, *J. Membr. Sci.*, 2004, **234**, 55.
6. C. P. Ribeiro, B. D. Freeman, D. S. Kalika and S. Kalakkunnath, *Ind. Eng. Chem. Res.*, 2013, **52**, 8906.
7. P. Rölling, M. Lamers and C. Staudt, *J. Membr. Sci.*, 2010, **362**, 154.
8. N. Wang, S. Ji, J. Li, R. Zhang and G. Zhang, *J. Membr. Sci.*, 2014, **455**, 113.
9. Q. F. An, J. W. Qian, Q. Zhao and C. J. Gao, *J. Membr. Sci.*, 2008, **313**, 60.
10. S. B. Kuila and S. K. Ray, *Sep. Purif. Technol.*, 2014, **123**, 45.
11. Y. Wang, S. Hirakawa, K. Tanaka, H. Kita and K. Okamoto, *J. Membr. Sci.*, 2002, **199**, 13.
12. A. Wolińska-Grabczyk, *J. Membr. Sci.*, 2006, **282**, 225.
13. F. Peng, L. Lu, H. Sun, Y. Wang, J. Liu and Z. Jiang, *Chem. Mater.*, 2005, **17**, 6790.
14. F. Peng, Z. Jiang, C. Hu, Y. Wang, L. Lu and H. Wu, *Desalination*, 2006, **193**, 182.
15. F. Peng, L. Lu, H. Sun, F. Pan and Z. Jiang, *Ind. Eng. Chem. Res.*, 2007, **46**, 2544.